Supporting Information

Boundaries of charge-discharge curves of batteries

Amir Haghipour [a], Maryam Tahertalari [b], Mohammad Mahdi Kalantarian,*[b]

[a.] *Materials Research Institute Aalen, Aalen University, Beethovenstr. 1, D-73430 Aalen, Germany.*
[b.] *Ceramic Department, Materials and Energy Research Center, P.O. Box 31787-316, Tehran, Iran.*
**Corresponding authors. E-mails: m.kalantarian@merc.ac.ir, kalantarian@gmail.com*

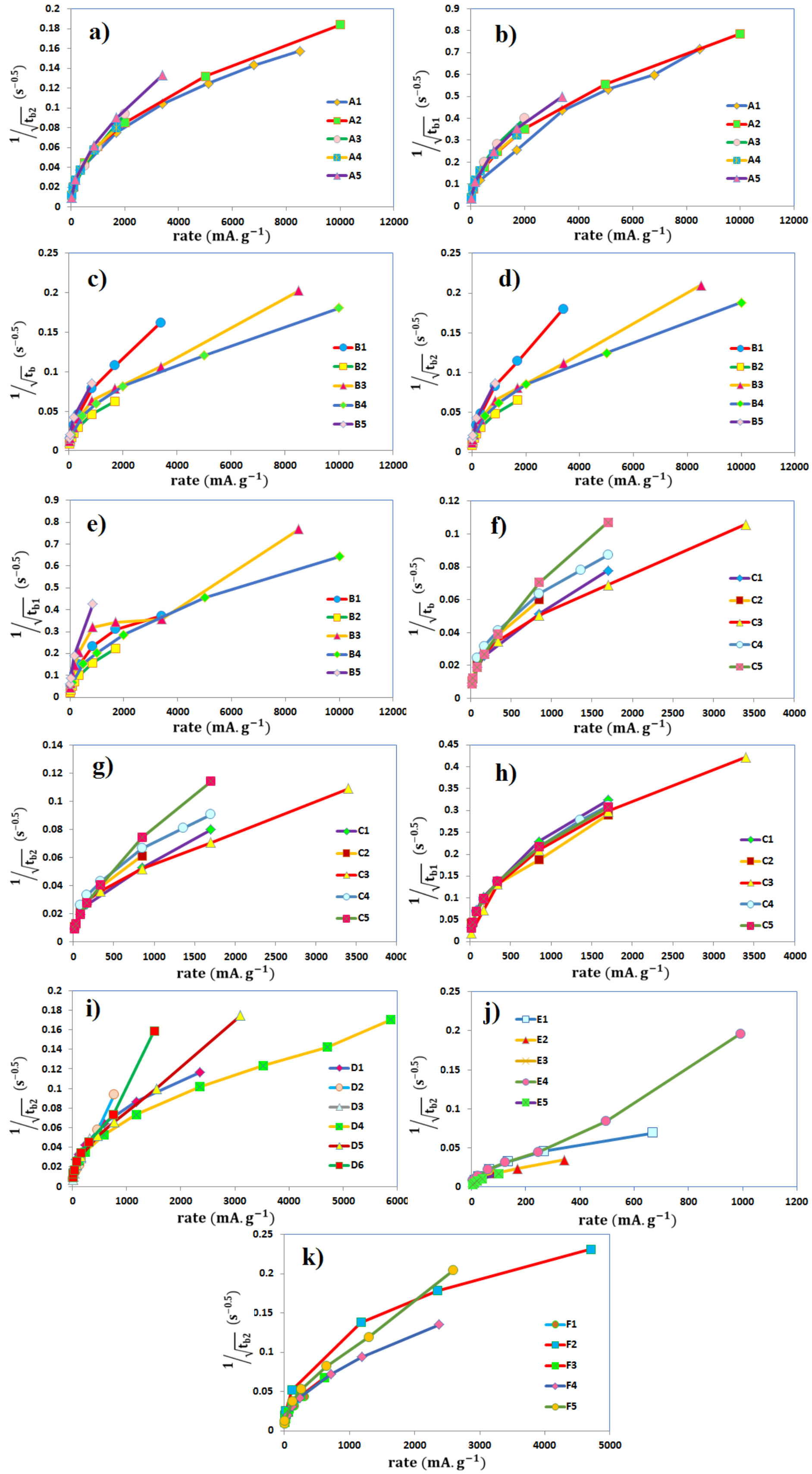

a)
b)
c)
d)
e)
f)
g)
h)
i)
j)
k)
rate (mA. g−1)
1/√tb2 (s−0.5)
1/√tb1 (s−0.5)
1/√tb (s−0.5)
A1
A2
A3
A4
A5
B1
B2
B3
B4
B5
C1
C2
C3
C4
C5
D1
D2
D3
D4
D5
D6
E1
E2
E3
E4
E5
F1
F2
F3
F4
F5

Figure S1. Plotting inverse value of the square root of t_b, t_{b1}, and t_{b2} (see Figure 3) for discharge V-T diagrams ($\frac{1}{\sqrt{t_b}}$) versus *rate* for several data taken from literature. The data are taken from discharge V-C diagrams of the following references: a and b) ultrafast charging and discharging $LiFe_{0.9}P_{0.95}O_{4-\delta}$ [1] (A1), semi-graphitic carbon-coated $LiFePO_4$ (LFP/C composite sample)[2] (A2), LFP/carbon nanocomposite with a core-shell structure[3] (A3), LFP/C nanocomposite using FePO4·2H2O nanoparticles (b-LFP sample)[4] (A4), carbon-coated LFP without use of sucrose during the synthesis (4-LFP3 sample)[5] (A5), c, d, and e) microspherical LFP-Carbon Composite[6] (B1), mesoporous LFP/C nano-composite with superior performance[7] (B2), LFP synthesized by a hydrothermal method with an average particle size of 200–300 nm and 3 wt% carbon coating on the particle surface (LFP sample)[8] (B3), core–shell LFP/carbon nanocomposite[9] (B4), porous nanostructured LFP powder synthesized without lauric acid[10] (B5), f, g, and h) porous nanostructured LFP powder synthesized with lauric acid[10] (C1), porous spherical LFP/C microscale composite[11] (C2), LFP/Graphene composite (LFP/G sample), LFP nanoparticles were synthesized using a hydrothermal method[12] (C3), micro dumbbell LFP[13] (C4), fractal LFP/C composite[14] (C5), i) nitrogen-doped carbon-wrapped $Na_3V_2(PO_4)_3/C$ (NVP/C/NC sample)[15] (D1), organic-electrolyte Na/$NaFePO_4$ cell[16] (D2), high performance $NaFePO_4$/C microsphere hybrid composite[17] (D3), hard carbon coated porous $Na_3V_2(PO_4)_3$@C composite (NVP@C@HC sample)[18] (D4), $NaFePO_4$ formed by aqueous ion-exchange[19] (D5), GO-wrapped $LiFeSO_4F$[20] (D6), j) monoclinic $Fe_2(SO_4)_3$ (M-$Fe_2(SO_4)$ [21] (E1), recovered nano-$LiMnPO_4$/C powder[22] (E2), Na/$NaFePO_4$ battery with reversible $NaFePO_4$ electrode[23] (E3), Na/carbon-coated Na_2FePO_4F synthesized by solid-state method[24] (E4), Carbon-coated $LiFeBO_3$ synthesized by sol-gel[25] (E5), k) PEDOT-$LiFeSO_4F$ composite[26] (F1), porous $Na_3V_2(PO_4)_3$/C cathode[27] (F2), porous sponge-like Na_2FePO_4F/C [28] (F3), Spoke-Like Nanorods of $Na[Ni_{0.61}Co_{0.12}Mn_{0.27}]O_2$ (SNA sample)[29] (F4), $Na_3V_2O_2(PO_4)_2F$ graphene sandwich structure[30] (F5).

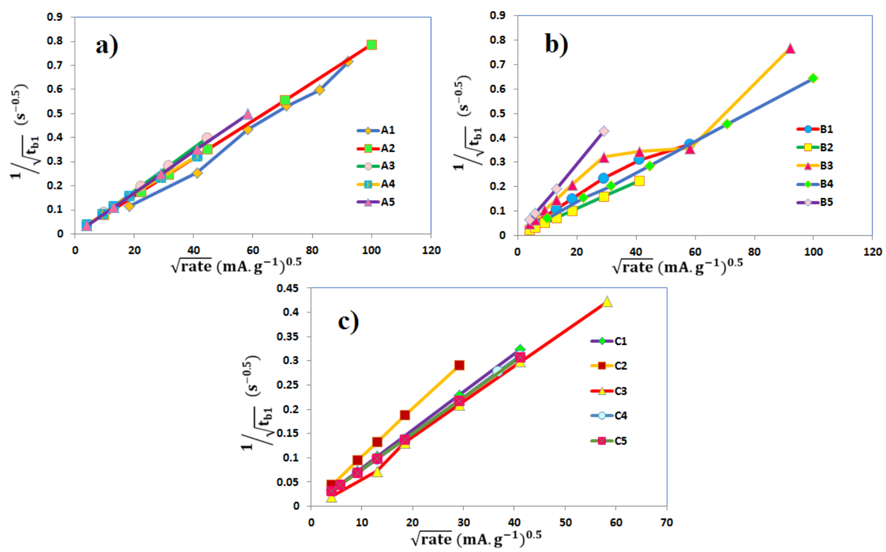

Figure S2. Plotting inverse value of the square root of t_{b1} (see Figure 3) for discharge V-T diagrams ($\frac{1}{\sqrt{t_b}}$) versus $\sqrt{rate}$ for several data taken from literature. The data are taken from discharge V-C diagrams of the following references: a) ultrafast charging and discharging $LiFe_{0.9}P_{0.95}O_{4-\delta}$ [1] (A1), semi-graphitic carbon-coated $LiFePO_4$ (LFP/C composite sample)[2] (A2), LFP/carbon nanocomposite with a core-shell structure[3] (A3), LFP/C nanocomposite using FePO4·2H2O nanoparticles (b-LFP sample)[4] (A4), carbon-coated LFP without use of sucrose during the synthesis (4-LFP3 sample)[5] (A5), b) microspherical LFP-Carbon Composite[6] (B1), mesoporous LFP/C nano-composite with superior performance[7] (B2), LFP synthesized by a hydrothermal method with an average particle size of 200–300 nm and 3 wt% carbon coating on the particle surface (LFP sample)[8] (B3), core–shell LFP/carbon nanocomposite[9] (B4), porous nanostructured LFP powder synthesized without lauric acid[10] (B5), c) porous nanostructured LFP powder synthesized with lauric acid[10] (C1), porous spherical LFP/C microscale composite[11] (C2), LFP/Graphene composite (LFP/G sample), LFP nanoparticles were synthesized using a hydrothermal method[12] (C3), micro dumbbell LFP[13] (C4), fractal LFP/C composite[14] (C5).

References:

1. B. Kang and G. Ceder, *Nature*, 2009, 458, 190-193.
2. Y. Wang, H. Li, P. He, E. Hosono and H. Zhou, *Nanoscale*, 2010, 2, 1294-1305.
3. Y. Wang, P. He and H. Zhou, *Energy & Environmental Science*, 2011, 4, 805-817.
4. C. Chen, G. Liu, Y. Wang, J. Li and H. Liu, *Electrochimica Acta*, 2013, 113, 464-469.
5. N. Kalaiselvi and A. Manthiram, *J. Power Sources*, 2010, 195, 2894-2899.
6. L. Yu, D. Cai, H. Wang and M.-M. Titirici, *Nanomaterials*, 2013, 3, 443-452.
7. G. Wang, H. Liu, J. Liu, S. Qiao, G. M. Lu, P. Munroe and H. Ahn, *Advanced Materials*, 2010, 22, 4944-4948.

8. H. Zheng, J. Li, X. Song, G. Liu and V. S. Battaglia, *Electrochimica Acta*, 2012, 71, 258-265.
9. H. Li and H. Zhou, *Chemical Communications*, 2012, 48, 1201-1217.
10. D. Choi and P. N. Kumta, *Journal of Power Sources*, 2007, 163, 1064-1069.
11. S. Ju, T. Liu, H. Peng, G. Li and K. Chen, *Materials Letters*, 2013, 93, 194-198.
12. X. Zhou, F. Wang, Y. Zhu and Z. Liu, *Journal of Materials Chemistry*, 2011, 21, 3353-3358.
13. L. Hu, T. Zhang, J. Liang, Y. Zhu, K. Zhang and Y. Qian, *RSC Advances*, 2016, 6, 456-463.
14. Z. Cabán-Huertas, O. Ayyad, D. Dubal and P. Gómez-Romero, 2016.
15. H.-b. Huang, S.-h. Luo, C.-l. Liu, Y. Yang, Y.-c. Zhai, L.-j. Chang and M.-q. Li, *Applied Surface Science*, 2019, 487, 1159-1166.
16. N. Wongittharom, T.-C. Lee, C.-H. Wang, Y.-C. Wang and J.-K. Chang, *Journal of Materials Chemistry A*, 2014, 2, 5655-5661.
17. S. Mukherjee, S. Bin Mujib, D. Soares and G. Singh, *Materials*, 2019, 12, 1952.
18. L. Chen, Y. Zhao, S. Liu and L. Zhao, *ACS applied materials & interfaces*, 2017, 9, 44485-44493.
19. W. Tang, X. Song, Y. Du, C. Peng, M. Lin, S. Xi, B. Tian, J. Zheng, Y. Wu and F. Pan, *Journal of Materials Chemistry A*, 2016, 4, 4882-4892.
20. Z. Guo, D. Zhang, H. Qiu, T. Zhang, Q. Fu, L. Zhang, X. Yan, X. Meng, G. Chen and Y. Wei, *ACS applied materials & interfaces*, 2015, 7, 13972-13979.
21. H. Park, J.-K. Yoo, W. Ko, Y. Lee, I. Park, S.-T. Myung and J. Kim, *Journal of Power Sources*, 2019, 434, 226750.
22. Q. Meng, J. Duan, Y. Zhang and P. Dong, *Journal of Industrial and Engineering Chemistry*, 2019, 80, 633-639.
23. S.-M. Oh, S.-T. Myung, J. Hassoun, B. Scrosati and Y.-K. Sun, *Electrochemistry communications*, 2012, 22, 149-152.
24. Y. Kawabe, N. Yabuuchi, M. Kajiyama, N. Fukuhara, T. Inamasu, R. Okuyama, I. Nakai and S. Komaba, *Electrochemistry Communications*, 2011, 13, 1225-1228.
25. W. Chen, L. Wu, X. Zhang, J. Liu, S. Liu and S. Zhong, *Journal of Solid State Electrochemistry*, 2018, 22, 1677-1687.
26. A. Sobkowiak, M. R. Roberts, R. Younesi, T. Ericsson, L. Häggström, C.-W. Tai, A. M. Andersson, K. Edström, T. r. Gustafsson and F. Björefors, *Chemistry of Materials*, 2013, 25, 3020-3029.
27. K. Saravanan, C. W. Mason, A. Rudola, K. H. Wong and P. Balaya, *Advanced Energy Materials*, 2013, 3, 444-450.
28. S. Hua, S. Cai, R. Ling, Y. Li, Y. Jiang, D. Xie, S. Jiang, Y. Lin and K. Shen, *Inorganic Chemistry Communications*, 2018, 95, 90-94.
29. J. Y. Hwang, S. T. Myung, C. S. Yoon, S. S. Kim, D. Aurbach and Y. K. Sun, *Advanced Functional Materials*, 2016, 26, 8083-8093.
30. M. Xu, L. Wang, X. Zhao, J. Song, H. Xie, Y. Lu and J. B. Goodenough, *Physical Chemistry Chemical Physics*, 2013, 15, 13032-13037.